REVIEW SUMMARY

OPTICS

# Lithium niobate photonics: Unlocking the electromagnetic spectrum

Andreas Boes*†, Lin Chang*†, Carsten Langrock, Mengjie Yu, Mian Zhang, Qiang Lin, Marko Lončar, Martin Fejer, John Bowers, Arnan Mitchell

**BACKGROUND:** Electromagnetic (EM) waves underpin modern society in profound ways. They are used to carry information, enabling broadcast radio and television, mobile telecommunications, and ubiquitous access to data networks through Wi-Fi and form the backbone of our modern broadband internet through optical fibers. In fundamental physics, EM waves serve as an invaluable tool to probe objects from cosmic to atomic scales. For example, the Laser Interferometer Gravitational-Wave Observatory and atomic clocks, which are some of the most precise human-made instruments in the world, rely on EM waves to reach unprecedented accuracies.

This has motivated decades of research to develop coherent EM sources over broad spectral ranges with impressive results: Frequencies in the range of tens of gigahertz (radio and microwave regimes) can readily be generated by electronic oscillators. Resonant tunneling diodes enable the generation of millimeter (mm) and terahertz (THz) waves, which span from tens of gigahertz to a few terahertz. At even higher frequencies, up to the petahertz level, which are usually defined as optical frequencies, coherent waves can be generated by solid-state and gas lasers. However, these approaches often suffer from narrow spectral bandwidths, because they usually rely on well-defined energy states of specific materials, which results in a rather limited spectral coverage.

To overcome this limitation, nonlinear frequency-mixing strategies have been developed. These approaches shift the complexity from the EM source to nonresonant-based material effects. Particularly in the optical regime, a wealth of materials exist that support effects that are suitable for frequency mixing. Over the past two decades, the idea of manipulating these materials to form guiding structures (waveguides) has provided improvements in efficiency, miniaturization, and production scale and cost and has been widely implemented for diverse applications.

**ADVANCES:** Lithium niobate, a crystal that was first grown in 1949, is a particularly attractive photonic material for frequency mixing because of its favorable material properties. Bulk lithium niobate crystals and weakly confining waveguides have been used for decades for accessing different parts of the EM spectrum, from gigahertz to petahertz frequencies. Now, this material is experiencing renewed interest owing to the commercial availability of thin-film lithium niobate (TFLN). This integrated photonic material platform enables tight mode confinement, which results in frequency-mixing efficiency improvements by orders of magnitude while at the same time offering additional degrees of freedom for engineering the optical properties by using approaches such as dispersion engineering. Importantly, the large refractive index contrast of TFLN enables, for the first time, the realization of lithium niobate–based photonic integrated circuits on a wafer scale.

**OUTLOOK:** The broad spectral coverage, ultralow power requirements, and flexibilities of lithium niobate photonics in EM wave generation provides a large toolset to explore new device functionalities. Furthermore, the adoption of lithium niobate–integrated photonics in foundries is a promising approach to miniaturize essential bench-top optical systems using wafer scale production. Heterogeneous integration of active materials with lithium niobate has the potential to create integrated photonic circuits with rich functionalities. Applications such as high-speed communications, scalable quantum computing, artificial intelligence and neuromorphic computing, and compact optical clocks for satellites and precision sensing are expected to particularly benefit from these advances and provide a wealth of opportunities for commercial exploration. Also, bulk crystals and weakly confining waveguides in lithium niobate are expected to keep playing a crucial role in the near future because of their advantages in high-power and loss-sensitive quantum optics applications. As such, lithium niobate photonics holds great promise for unlocking the EM spectrum and reshaping information technologies for our society in the future. ■

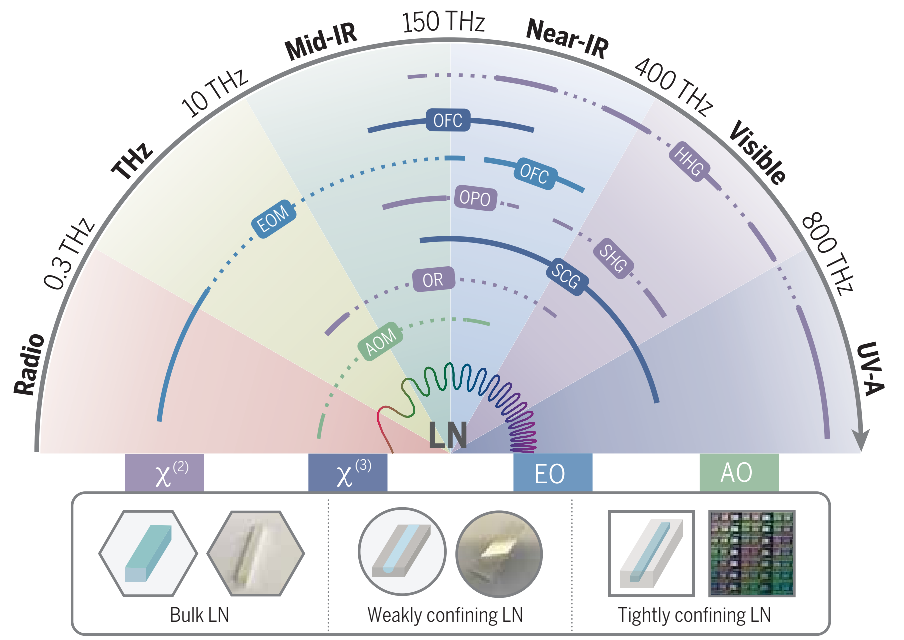


**Lithium niobate spectral coverage.** The EM spectral range and processes for generating EM frequencies when using lithium niobate (LN) for frequency mixing. AO, acousto-optic; AOM, acousto-optic modulation; $\chi^{(2)}$, second-order nonlinearity; $\chi^{(3)}$, third-order nonlinearity; EO, electro-optic; EOM, electro-optic modulation; HHG, high-harmonic generation; IR, infrared; OFC, optical frequency comb; OPO, optical paramedic oscillator; OR, optical rectification; SCG, supercontinuum generation; SHG, second-harmonic generation; UV, ultraviolet.

The list of author affiliations is available in the full article online.
*Corresponding author. Email: andy.boes@adelaide.edu.au (A.B.); linchang@pku.edu.cn (L.C.)
†These authors contributed equally to this work.
Cite this article as A. Boes *et al.*, *Science* 379, eabj4396 (2023). DOI: 10.1126/science.abj4396

READ THE FULL ARTICLE AT
https://doi.org/10.1126/science.abj4396

REVIEW

OPTICS

# Lithium niobate photonics: Unlocking the electromagnetic spectrum

**Andreas Boes[1,2,3]*†, Lin Chang[4,5]*†, Carsten Langrock[6]‡, Mengjie Yu[7,8], Mian Zhang[9], Qiang Lin[10], Marko Lončar[7], Martin Fejer[6], John Bowers[11], Arnan Mitchell[1]**

**Lithium niobate (LN), first synthesized 70 years ago, has been widely used in diverse applications ranging from communications to quantum optics. These high-volume commercial applications have provided the economic means to establish a mature manufacturing and processing industry for high-quality LN crystals and wafers. Breakthrough science demonstrations to commercial products have been achieved owing to the ability of LN to generate and manipulate electromagnetic waves across a broad spectrum, from microwave to ultraviolet frequencies. Here, we provide a high-level Review of the history of LN as an optical material, its different photonic platforms, engineering concepts, spectral coverage, and essential applications before providing an outlook for the future of LN.**

The technological development of our modern society is closely linked to our ability to make use of electromagnetic (EM) waves. The wide EM spectrum, spanning from radiowaves and microwaves through infrared radiation, visible light, and ultraviolet (UV) radiation up to high-energy x- and $\gamma$-rays, has transformed the way we record images, carry information, and transmit energy. Driven by the sophisticated control of EM waves, the past few decades have witnessed notable breakthroughs in a wide range of areas such as high-speed communication (*1*, *2*), ultraprecision time-frequency metrology (*3*–*5*), bioimaging (*6*–*8*) and quantum-information science (*9*, *10*).

The generation and manipulation of EM waves lies at the heart of all scientific and technological explorations. Depending on the frequencies, there are several main strategies for generation and processing: Radio frequency (RF) (<~100 GHz) signals can readily be produced by microwave oscillators and then manipulated through conventional complementary metal-oxide-semiconductor (CMOS) electronics. Signals with frequency greater than 100 GHz (typically referred to as millimeter waves) up to a few THz can be generated, for example, by resonant tunneling diodes and processed by high-speed electronics that use silicon or III-V semiconductors. For higher frequencies (10 THz to 1 PHz) in the optical regime, the most common methods for EM wave generation use solid-state, fiber, gas, and semiconductor lasers. Although these strategies have successfully enabled many applications, each platform individually can only offer a limited spectral coverage because of the specific platform's dependence dependence on well-defined energy bands or levels of solid-state materials, atoms, and molecules.

To overcome this limitation, another important strategy, parametric nonlinear frequency mixing, was introduced. Starting from optical frequencies (hundreds of THz), this process leverages broadband parametric nonlinear effects for multiwave mixing to unlock previously inaccessible EM frequencies on demand. This approach shifts the complexity from a custom EM wave source to nonresonant material effects, which can be engineered with additional degrees of freedom, allowing access to a much broader part of the EM spectrum (THz to PHz) with unprecedented control and performance. In addition to nonlinear frequency mixing, the GHz to THz part of the EM spectrum can be bridged through microwave-to-optical conversion, enabling the efficient processing of EM waves through well-established CMOS electronics.

These prospects spurred the development of a wide range of nonlinear and electro-optic material platforms over the past few decades. Among these platforms, lithium niobate ($LiNbO_3$, or LN), which has been described as the "the silicon of photonics" (*11*), turns out to be particularly suitable for the generation and manipulation of EM frequencies because it offers a rare combination of advantageous properties: (i) large electro-optic, piezoelectric, and nonlinear-optic material coefficients; (ii) engineerability of velocity matching through quasi–phase matching (QPM) and waveguide dispersion; (iii) broad transparency (400 nm to 5 μm); (iv) long-term stability; and (v) widespread commercial availability of large, low-cost, optical-quality wafers. This makes LN one of the key photonic materials that has the potential to expand access to an ultrawide part of the EM spectrum and support the next generation of scientific breakthroughs and commercial products.

## LN platforms

LN is a ferroelectric crystal and was first synthesized in 1949 (*12*) in its polycrystalline form. From this discovery, it took 15 years until further studies identified the material's characteristic electro-optical (*13*) and second-order nonlinear-optical (*14*) properties. The growth of single-crystalline LN using the Czochralski technique (*15*, *16*) represented a breakthrough; this technique is still in use today and is able to produce optical-quality wafers up to a diameter of 150 mm (6 inches), and several crystal compositions—such as congruent, near-stoichiometric, or doped with alkaline or transition metals—are available commercially. Over the decades, three main LN photonic platforms have emerged, namely bulk crystals, weakly confining waveguides, and tightly confining waveguides, whose evolution can be found in Fig. 1.

### *Bulk LN crystals*

Bulk LN crystals have found wide adoption for generation and manipulation of EM waves owing to their compatibility with free-space optical setups, ability to handle high optical power, ease of fabrication, and low cost. Such crystals are typically millimeter- to centimeter-scale blocks of LN with optical-grade polished facets (see right side of Fig. 1).

Early demonstrations in bulk LN crystals include electro-optic modulation (*13*) and second-harmonic generation (SHG) (*14*). A breakthrough discovery occurred when it was observed that the spontaneous polarization of LN crystals could be inverted locally by applying a high electric field at room temperature (*17*). This process, referred to as "electric-field poling," opened a reliable path for engineering the phase-velocity matching (i.e., momentum conservation) between different waves and made previously explored domain-inversion methods that relied on high-temperature ionic diffusion processes (*18*) obsolete. Photorefraction was first discovered when investigating LN for nonlinear devices (*19*), which later provided the means for high-density data storage in LN (*20*).

[1]Integrated Photonics and Applications Centre (InPAC), School of Engineering, RMIT University, Melbourne, VIC 3000, Australia. [2]Institute for Photonics and Advanced Sensing (IPAS), University of Adelaide, Adelaide, SA 5005, Australia. [3]School of Electrical and Electronic Engineering, University of Adelaide, Adelaide, SA 5005, Australia. [4]State Key Laboratory of Advanced Optical Communications System and Networks, School of Electronics, Peking University, Beijing 100871, China. [5]Frontiers Science Center for Nano-optoelectronics, Peking University, Beijing 100871, China. [6]Edward L. Ginzton Laboratory, Stanford University, Stanford, CA 94305, USA. [7]John A. Paulson School of Engineering and Applied Sciences, Harvard University, Cambridge, MA 02138, USA. [8]Ming Hsieh Department of Electrical and Computer Engineering, University of Southern California, Los Angeles, CA 90089, USA. [9]HyperLight, Cambridge, MA 02139, USA. [10]Department of Electrical and Computer Engineering, University of Rochester, Rochester, NY 14627, USA. [11]Department of Electrical and Computer Engineering, University of California, Santa Barbara, CA 93106, USA.
*Corresponding author. Email: andy.boes@adelaide.edu.au (A.B.); linchang@pku.edu.cn (L.C.) †These authors contributed equally to this work. ‡Present address: Keysight Laboratories, Santa Clara, CA 95952, USA.

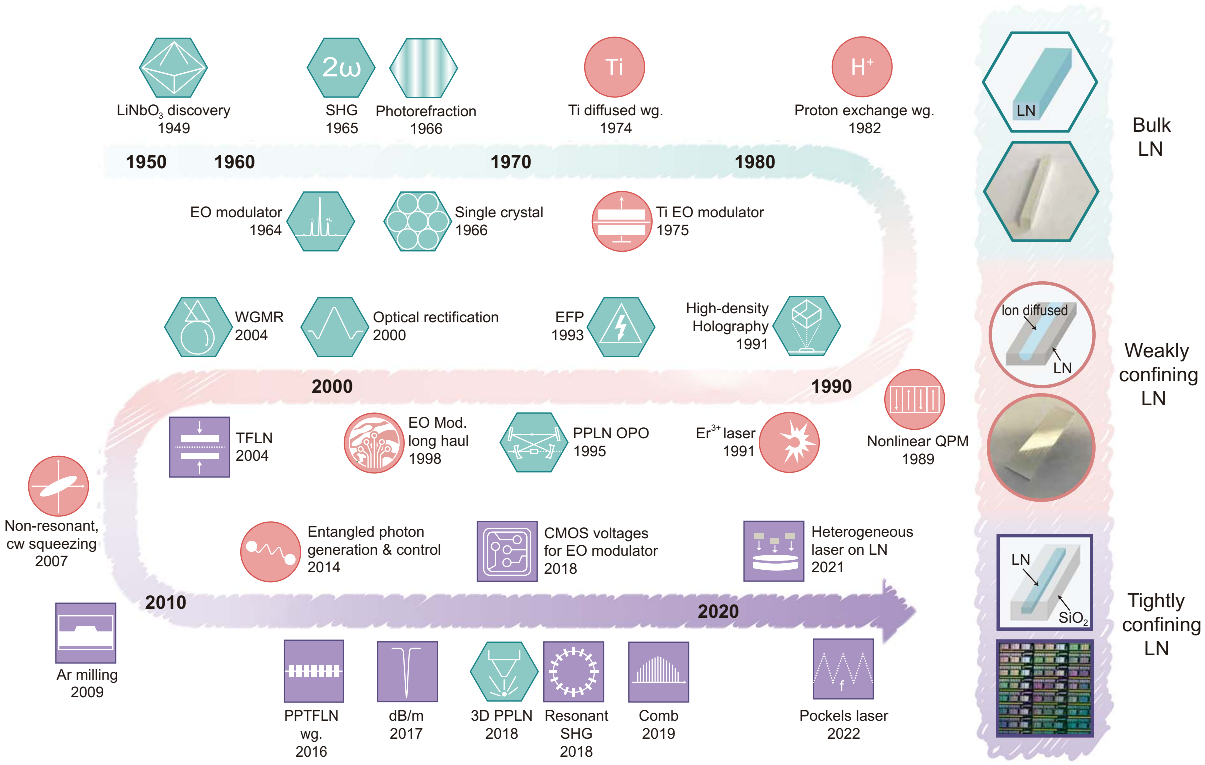


**Fig. 1. Timeline of LN as a photonic material.** LN has been developed into three major platforms: bulk crystals, weakly confining waveguides, and tightly confining waveguides (indicated by blue, pink, and purple, respectively). Milestone demonstrations are highlighted. cw, continuous-wave; EO, electro-optic; wg., waveguide; EFP, electric-field poling; WGMR, whispering gallery resonator; PPTFLN, periodically poled thin film LN.

Bulk crystals have also been formed in the shape of discs or ring cavities, by careful polishing of their facets (*21*–*23*). Such discs can form so-called whispering gallery resonators (*24*), with quality factors reaching hundreds of millions (*25*), making them attractive for highly coherent optical wave or microwave sources and nonlinear-optical applications. Recently, it was shown that ferroelectric domain engineering can also be achieved in three dimensions by using femtosecond laser pulses that are focused into the crystal (*26*). This demonstration opens opportunities for a new class of wave-mixing devices that were not previously feasible, such as three-dimensional nonlinear photonic crystals.

Bulk crystals are particularly attractive in optical cavity configurations such as parametric oscillators (*27*, *28*) (see Fig. 2) to enhance the nonlinear interaction. They are also attractive for high-power applications, for use inside laser cavities (Q-switch, intracavity SHG), or when using ultrashort, high–peak power laser pulses.

### *Weakly confining LN waveguides*

Weakly confining LN waveguides maintain interacting fields over centimeter-length distances in small-mode volumes at high intensities (Fig. 1), thereby increasing nonlinear mixing efficiencies by two to three orders of magnitude when compared with bulk crystals. This relaxes the optical power requirements and enables efficient EM wave generation at moderate optical powers in the range of milliwatts (continuous-wave) or few nanojoules (pulsed).

Weakly confining LN waveguides can be formed by slightly altering the material composition or structure to locally increase the refractive index to form the guiding core. The first weakly confining waveguides were demonstrated by lithium out-diffusion (*29*), which was followed shortly thereafter by titanium in-diffusion (*30*) and later proton exchange (*31*) and femtosecond laser writing (*32*). Titanium in-diffusion and proton exchange remain common fabrication methods and require increased temperatures to drive the diffusion processes (~1100°C for titanium in-diffusion and ~200°C for proton exchange), which increase the extraordinary refractive index of LN by a few times $10^{-3}$ (*33*) and ~0.1 (*34*), respectively. To form low-loss, nonlinear-active waveguides through proton exchange, an annealing step at ~300°C is used, which reduces the index contrast to ~0.02. Such waveguides have been used for a number of frequency-mixing demonstrations such as the first implementation of QPM (see Fig. 3) for SHG in LN (*35*, *36*) and integrated erbium lasers (*37*). Importantly, when used as low-loss, high-speed electro-optic modulators, such waveguides were a key component for long-haul communication systems (*38*). This platform has been explored for low-loss quantum-optical applications, for example, up-conversion to near-visible wavelengths for single-photon detection (*39*) and on-chip entangled photon-pair generation by spontaneous parametric down-conversion and control of the generated photons (*40*). A large body of work in this field is reviewed in Gil-Lopez *et al.* (*41*).

Weakly confining waveguides are attractive because their mode volume is naturally close to that of standard optical fibers, which enables low interface losses (<0.5 dB at near-infrared wavelengths) between waveguide and fiber. Thus, a wide range of optical equipment that has been developed for high-speed optical communication can readily be connected to these waveguides, providing a large range of linear and nonlinear optical signal processing functionalities (*42*). These waveguides can be inexpensively produced on a wafer scale and only require standard lithographic tools with readily available micrometer resolution.

### *Tightly confining LN waveguides*

Tightly confining LN waveguides are a relatively new class of LN structures with even smaller mode volumes that reach subwavelength mode

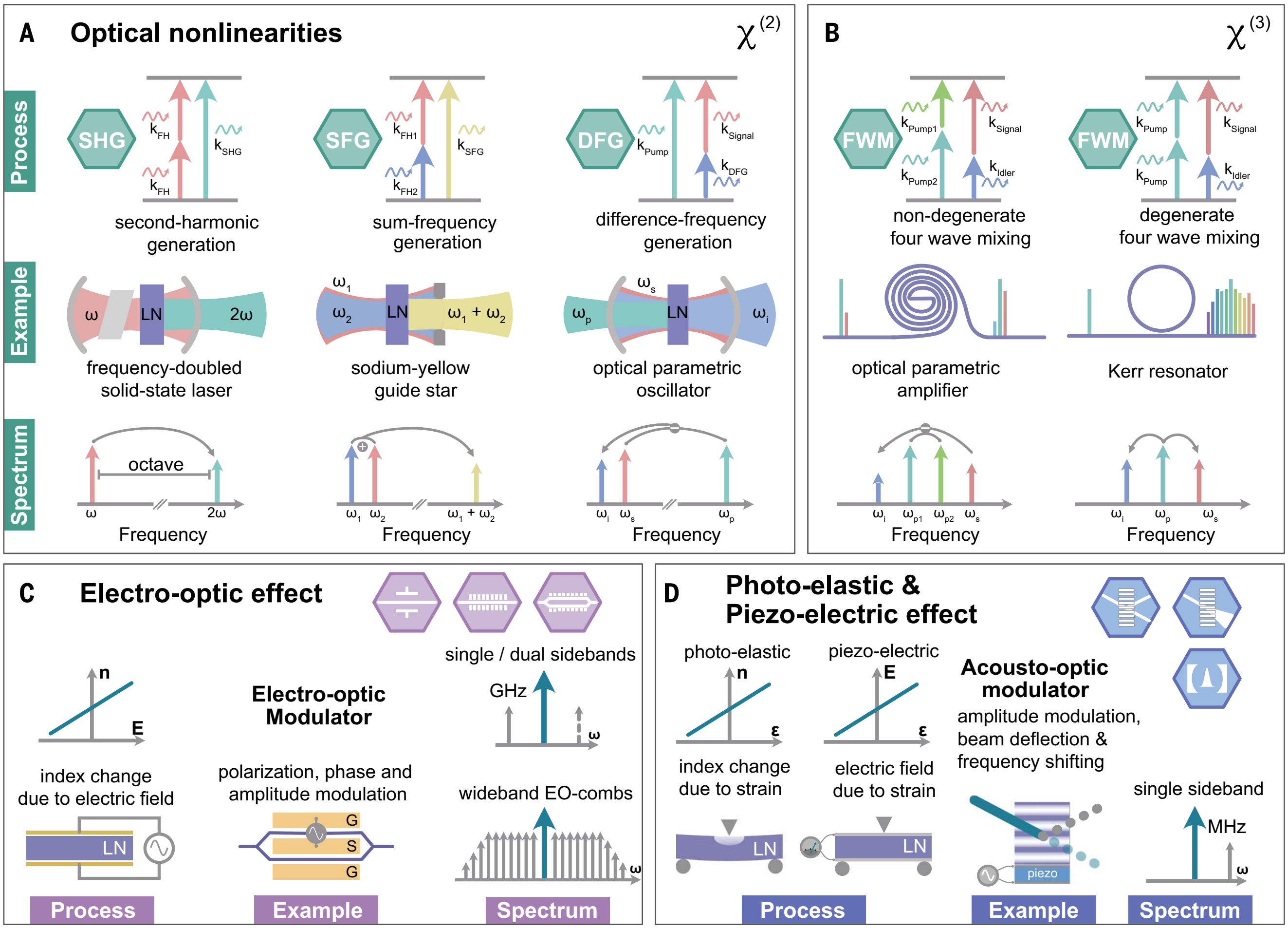


**Fig. 2. LN material properties used for generating and manipulating EM waves.** (**A** to **D**) Illustration of the (A) second-order and (B) third-order nonlinear-optic, (C) electro-optic, and (D) photo-elastic and piezo-electric material properties of LN that are used for efficient generation and manipulation of EM frequencies on demand.

diameters. This results in frequency mixing efficiencies that are nearly two orders of magnitude higher than those of weakly confining waveguides, in addition to offering broad integration and dispersion-engineering opportunities.

Such strongly confining waveguides (43) use a thin film of LN on a lower-index cladding layer, akin to the silicon-on-insulator platform, which can be manufactured at scale with good film uniformity and quality. Optical waveguides are typically made by dry etching (44) the LN film to form ridge waveguides or by strip-loading with a material that has a refractive index that is higher than that of the top cladding (45); however, methods such as laser ablation and diamond-blade scoring have also been explored. The optical modes in such waveguides are tightly confined because of the subwavelength waveguide dimensions and the high refractive index contrast between the guiding core and cladding, which enables dense integration using low-loss small-radius bends (46). This high index contrast has led to highly efficient and compact frequency-mixing and frequency-generating components such as frequency doublers (45, 47, 48), electro-optic modulators (49, 50), optical frequency comb (OFC) generators (51–53), and lasers and amplifiers based on Er doping (54, 55).

The thin-film LN (TFLN) platform enables photonic integration at a scale and density approaching that available on semiconductor platforms (56). This is a highly attractive proposition because the material properties of LN allow for the homogeneous integration of important active and passive photonic functions, often eliminating the need for additional materials. To incorporate lasers and detectors on TFLN, building blocks based on III-V semiconductor materials still require heterogeneous integration (57), which may be accomplished using techniques developed for other popular integrated-photonic platforms such as silicon and silicon nitride (58).

Because TFLN combines high confinement and high nonlinearity, it is particularly suitable for low-power continuous-wave and low-energy pulsed applications (59). For high-power or high-energy pulsed excitation, confinement or nonlinearity are less critical, and many other bulk materials such potassium titanyl phosphate (KTP) and β-$BaB_2O_4$ (BBO) are frequently used. However, one advantage of thin-film platforms, such as TFLN, over bulk solutions is the flexibility of engineering the waveguide geometry, and hence dispersion, which results in greater flexibility of phase and group velocity matching, enabling tailoring of components within integrated systems to access previously unachievable operating regimes.

## Material properties and engineering concepts for bridging the EM spectrum

LN is one of several materials that has many attractive properties for generating and manipulating EM waves, including large nonlinear-optic, electro-optic, and piezo-electric coefficients, as illustrated in Fig. 2. LN can also support various engineering concepts to further enhance these effects, as shown in Fig. 3.

### *Nonlinear-optical effects*

Nonlinear-optical effects can be used to generate new EM waves through second-order [$\chi^{(2)}$] and third-order [$\chi^{(3)}$] nonlinear-optical processes.

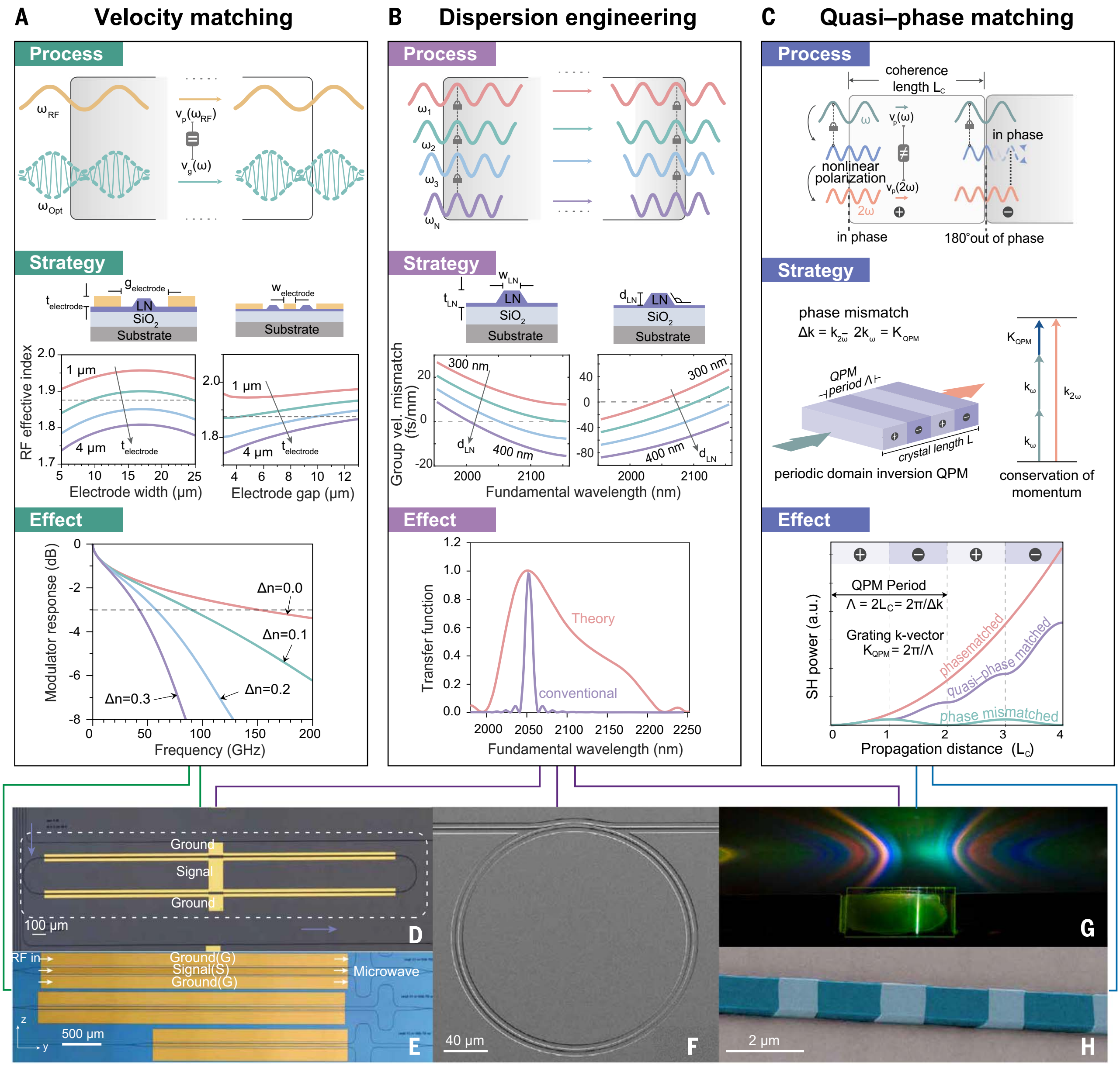


**Fig. 3. Engineering concepts used in LN technology to enable efficient coupling for a wide spectral range.** (**A** to **C**) Some of the most commonly used concepts in LN technology include the following: (i) Velocity matching (A) for broadband electro-optic interaction. Broadband electro-optic modulators can be realized by engineering the electrode dimensions to achieve velocity matching between the phase velocity of a single-frequency RF signal and the group velocity of the optical wave. (ii) Dispersion engineering (B) for broadband nonlinear optic interaction. Broadband nonlinear optical interaction can be realized by engineering the waveguide dimension to achieve low group velocity (vel.) mismatch. (iii) QPM (C) for efficient second-order nonlinear interaction. Phase mismatch between the interaction waves can be compensated to achieve efficient nonlinear optical interaction by inverting LN's spontaneous polarization periodically. a.u., arbitrary units. (**D**) EO comb generators that leverage velocity matching and dispersion engineering. [Reprinted by permission from Springer Nature Customer Service Centre GmbH: Springer *Nature* (53), 2019]. (**E**) High-speed EO modulators that leverage velocity matching. [Reprinted by permission from Springer Nature Customer Service Centre GmbH: Springer *Nature* (49), 2019]. (**F**) A Kerr microcomb generator that leverages dispersion engineering. [Reprinted with permission from (52) © The Optical Society]. (**G**) SHG waveguides that leverage dispersion engineering and QPM. [Reprinted with permission from (59) © The Optical Society]. (**H**) An SHG waveguide that leverages QPM. [Reprinted with permission from (144) © The Optical Society].

Below the Curie temperature of LN (1150°C), its crystal structure is noncentrosymmetric, giving rise to a large second-order nonlinearity. Meaning that an EM wave polarized along one crystal axis can cause a phase shift in another EM field with a certain polarization. The full set of such interactions is called the nonlinear tensor. For LN the strongest component is where both EM waves are polarized along the axis of crystal asymmetry(termed $d_{33}$) and is 27 pm/V at 1064 nm. Common second-order nonlinear processes include SHG, sum-frequency generation (SFG), and difference-frequency generation (DFG) (Fig. 2A). Third-order nonlinear optical processes in LN use its nonlinear refractive index ($n_2$) of 1.8 × $10^{-19}$ $m^2$/W (60), which is similar in strength to that of $Si_3N_4$ (2.5×$10^{-19}$ $m^2$/W at 1.55 μm), enabling efficient four-wave mixing processes that are suitable for applications such as optical frequency comb (Fig. 2B).

### *Linear electro-optic effect*

The linear electro-optic effect (or Pockels effect) changes the refractive index of LN proportional to an applied electric field, which can be used to modulate EM waves that pass through the crystal, generating new frequencies around the injected wave spaced by a single or multiple of the electrical modulation frequency (Fig. 2C). LN's largest electro-optic coefficient is crystal-axis dependent (closely related to the nonlinear tensor) with the largest component being on the order of 30 pm/V and typically requires interaction lengths of several millimeters up to a few centimeters to achieve the desired phase shifts with reasonably low voltages. The effect has been used to modulate and manipulate EM waves with electrical signals from static or very low frequency to hundreds of gigahertz. A key advantage of LN is that the electro-optic effect only changes the phase of light with no change to absorption. This is in contrast to silicon and other semiconductors where it is difficult to achieve independent phase and amplitude control.

### *Photo-elastic effect*

The photo-elastic effect changes the refractive index of LN as a function of strain, which can be used for modulating and frequency-shifting EM waves by interacting with periodically sheared or compressed LN caused by the excitation of acoustic waves via the piezoelectric effect (Fig. 2D). Typically, operation frequencies of acousto-optical devices in LN are in the megahertz to single-digit gigahertz range, mainly because of practical considerations such as the size of the crystal and manufacturability of the electrodes.

## Advantages of LN

A more detailed description of these effects and their use in LN can be found in several other review papers (*60–65*). Important to note is that LN does not necessarily exhibit the strongest material effects when compared with other materials. Indeed, there are many other materials such as KTP, BBO, GaAs, and InP that have attractive material properties. However, LN distinguishes itself by its maturity, stability, commercial availability, wide transparency range, and engineerability with respect to the coupling between EM frequencies within a wide spectral range, making their generation more efficient and tailorable.

### *Velocity matching*

Velocity matching is used for one of the most common optical components in LN, namely broadband electro-optic traveling-wave modulators (Fig. 3A). For efficient electro-optic interaction of the RF wave with the optical wave, the phase velocity of the single-frequency RF wave and the group velocity of the optical wave should ideally be identical. This can be achieved by engineering waveguide and electrode dimensions as well as material dispersion. In the weakly confined LN waveguide platform, the relatively high dielectric constant ($\xi_{11,22}$ = 44, $\xi_{33}$ = 27.9) of LN at microwave frequencies results in a velocity mismatch, which can be addressed by using thick electrodes (a few micrometers) to increase the phase velocity of the RF wave. The lower dielectric constant of $SiO_2$, which is a common buffer layer for tightly confining waveguides, increases the phase velocity of the RF wave, overcoming the need for thick electrodes for velocity matching.

### *Dispersion engineering*

Dispersion engineering uses the material stack and waveguide dimensions as degrees of freedom to engineer the modal dispersion. Waveguide dispersion is determined by the wavelength-dependent field distribution in the core and cladding of the waveguide (Fig. 3B). This waveguide (or geometric) dispersion can become an important factor in the overall dispersion, otherwise solely determined by the material properties, by providing control over the group-velocity mismatch and group-velocity dispersion (*59*, *66*). Within the LN platforms mentioned above, meaningful dispersion engineering is usually only available in TFLN because of the large index contrast between core and cladding.

### *QPM*

QPM is a technique that compensates for the phase-velocity (i.e., momentum) mismatch of different waves. This can be achieved by either periodically inverting the spontaneous polarization of the crystal when the phase mismatch reaches 180° [after a distance called the coherence length $L_C$ (*17*)] (Fig. 3C) or, in guided-wave platforms, by periodically perturbing the magnitude of the nonlinear coupling through modifications of the waveguide dimensions (*67*). In the small signal conversion regime, this results in a unidirectional energy flow over the entire propagation length. The periodic reversal of the spontaneous polarization can be achieved by using well-developed optical, thermal, and electrical domain-engineering methods (*68*), among which the electric-field poling method is the most widely adopted one and has been applied to all three LN platforms to generate periodically and aperiodically poled LN crystals with periods reaching submicron dimensions (*69*). Because of the Fourier-transform relationship between the QPM grating and the device's transfer function (*70–72*), a nontrivial frequency response can also be readily engineered (*73*). It is important to note that electric-field poling and QPM engineerability are not available in most other optical material platforms, which is one of the main reasons for the wide adoption of LN for nonlinear optical applications.

## LN photonics for unlocking the EM spectrum

LN's combination of material properties and engineerability provides the means to generate EM frequencies over a range that covers nearly five orders of magnitude (*53*, *74–77*), spanning from UV light to microwaves. Figure 4 illustrates the breadth of frequencies that have been experimentally generated and manipulated using LN as a linear and nonlinear frequency-mixing platform.

### *Visible and UV light*

Visible and UV light (400 to 900 THz) experiences very low material losses in LN owing to the 3.93-eV-wide bandgap (~950 THz) (*78*) of LN. Light in this spectral range is required for applications such as virtual reality (*79*) and probing atomic transitions for optical clocks or magnetic field sensors (*80*), as well as for molecules and cells for bioimaging (*6*). Visible frequencies can be generated in LN by making use of the material's second- and third-order optical nonlinearities in combination with well-developed near-infrared light sources. For example, the second-order optical nonlinearity has enabled the generation of blue (*17*, *81–83*), green (*82*, *84*), yellow (*82*), orange (*82*, *85*), and red (*82*) frequencies by using either SHG, which increases the EM frequency by one octave; SFG; or a combination thereof. The highest EM frequencies that can be generated by such nonlinear optical processes are only limited by the UV absorption edge of LN (~950 THz, or 315 nm) and can reach up to 800 to 900 THz (*77*, *82*) in the near UV spectral range.

Supercontinuum generation (SCG) provides another means to generate visible light in LN by generating EM frequencies over a very broad spectral bandwidth that possibly covers the entire visible spectrum and can reach all the way to 850 THz (*59*, *76*, *86*). SCG typically uses the third-order nonlinearity in dispersion-engineered waveguides. However, in LN, the second-order optical nonlinearity can further help to push the generated spectrum toward shorter wavelengths through SHG and SFG (*76*). Furthermore, the cascading of two second-order processes can result in a large effective third-order nonlinearity, which exceeds the material's third-order nonlinearity and whose sign can be controlled through the choice of the sign of the phase mismatch. (*87*, *88*).

### *Near-infrared frequencies*

Near-infrared frequencies (150 to 400 THz) are of particular interest because they are low enough for Rayleigh scattering to be minimal but high enough such that molecular absorption can be avoided in specific windows, which enables low loss transmission through optical fibers and on photonic integrated circuits (PICs). This makes them particularly attractive for applications such as optical communications (*1*, *2*), microwave photonics (*89*), and quantum

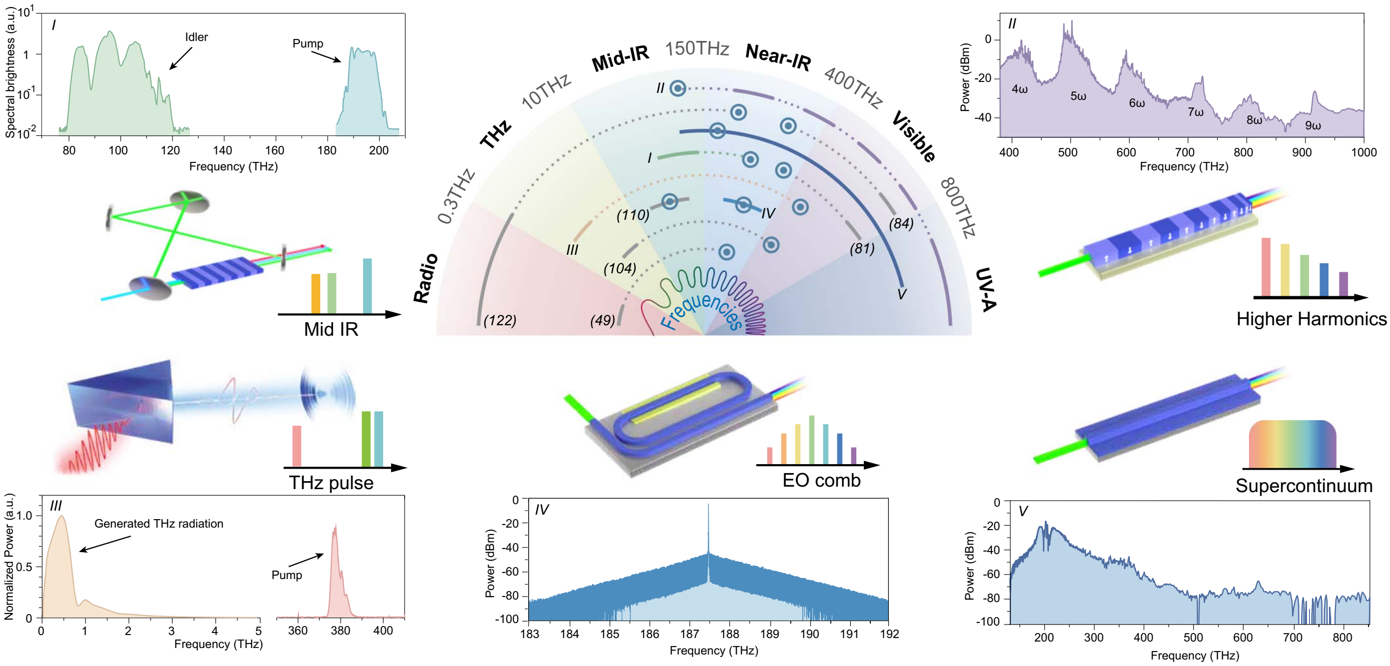


**Fig. 4. LN spectral coverage.** The semicircle illustrates the EM spectrum range and examples of generated EM frequencies when using LN for frequency mixing, with I to V representing OPO mid–infrared (IR) (I), higher harmonic (II), THz (III), EO comb (IV), and supercontinuum (V) generation [see (49, 81, 84, 104, 110, 122) for examples]. The circled dots in the spectrum indicate the pump frequency. The illustrations and the detailed spectra surrounding the semicircle (from left to right, top to bottom) provide examples for (IR) (I) (74), (II) (77), (III) (75), (IV) (53), and (V) (76).

optics (9, 10), as well as for free-space applications that operate outside the visible spectrum, such as light detection and ranging (LiDAR) and deep-space communication (90). Depending on the application, near-infrared frequencies can be generated in LN through a wide range of approaches, including Raman lasing and DFG, which are processes that generate one or two new EM frequencies, as well as Kerr microcombs, SCG, and electro-optic combs, which can generate tens to hundreds of new EM frequencies in the form of OFCs. For example, the generation of photons at 185 THz was demonstrated using Raman lasing in a high–Q-factor TFLN resonator (91) pumped at 192 THz. A popular approach for the generation of widely tunable EM frequencies is the use of an optical parametric oscillator (OPO). Here, two EM waves are generated, the signal and idler, which can be tuned by adjusting the phase-matching condition to enable the generation of frequencies between 200 and 268 THz (signal) and 110 and 178 THz (idler) (92). Such OPOs, operating with either continuous-wave or pulses of light, are commercially available and offer wide spectral tunability, which is difficult to achieve by other means. Squeezed light sources have also been demonstrated in the near-infrared spectral range as fundamental building blocks for quantum sensing and computing using degenerate parametric down conversion (93–95).

Applications that require the generation of many closely spaced EM frequencies can use OFCs. These combs have been demonstrated at near-infrared wavelengths using high–Q-factor, dispersion-engineered Kerr micro resonators in TFLN (51, 52, 96), which use the third-order optical nonlinearity of LN or cascaded second-order optical nonlinearities (97). Optical pump frequencies in the center of the C-band (~192 THz) are often used because of the availability of inexpensive light sources, such as narrow-linewidth and mode-locked lasers and high-power fiber amplifiers. An alternative way to generate near-infrared wavelengths is to use SCG (similar to the process outlined for visible-frequency generation), which has been used for generating OFCs that cover the full near-infrared frequency range and even reach into the visible (600 THz) and mid-infrared (100 THz) regions (59, 98). Electro-optic combs provide another powerful tool to generate OFCs—hundreds of comb lines from 183 to 192 THz spaced by 25 GHz have been demonstrated (53, 99–101).

### *Mid-infrared frequencies*

Mid-infrared frequencies (10 to 150 THz) experience low losses in LN for frequencies above ~55 THz, when the phonon absorption starts to take place (102). Mid-infrared frequencies are attractive because they can be used to excite vibrational states of molecules (103) and hence are useful sources for spectroscopic sensors in applications such as air-quality monitoring in cities or for process monitoring of chemical plants and emissions from pipelines. Such frequencies have historically been generated in OPOs by using bulk periodically poled LN (PPLN) crystals. Use of this process has enabled the generation of EM waves from near-infrared frequencies down to 56 THz in the mid-infrared region (104–106), which is at the edge of the transparency window of LN. More recently, mid-infrared frequencies generated by DFG have been demonstrated in weakly confining (107, 108) as well as TFLN waveguides, with continuous wave conversion efficiencies improving by one to two orders of magnitude. TFLN waveguides can also be used to efficiently translate near-infrared frequency combs to the mid-infrared region owing to the large conversion bandwidth afforded by dispersion engineering (109).

Kerr microcombs (110) and SCG (98, 111) have both been used to generate OFCs in the mid-infrared region, with the former relying on high–Q-factor TFLN ring resonators to generate an OFC from 139 to 162 THz (96). The frequency combs generated by SCG have a wider spectral width and can reach all the way to 60 THz (111), a value limited by the phonon absorption of LN. In the TFLN platform, the material absorption of the silica cladding layer underneath the LN thin film can also limit the generated frequencies, which has recently been overcome by using sapphire as a low-index cladding material (109) or by undercutting the waveguide region (112).

### *THz frequencies*

THz radiation (0.3 to 10 THz) can penetrate paper, plastics, and fabric and is therefore attractive for standoff sensing and security imaging, such as at airports. LN crystals are attractive for the generation of narrow-band, high-intensity THz frequencies by optical rectification, which is a second-order nonlinear-optic process and can also be described by intrapulse DFG. In this process, the spectral frequency components of ultrashort optical pump pulses interact with each other and generate new EM-frequency components. This process can generate frequencies up to the difference between the blue and red edges of the pulse spectrum, so that a 10-fs pulse centered at 800 nm, for example, could generate frequencies up to ~44 THz (6.8 μm).

The pump pulses that have been used for optical rectification in bulk LN crystals are in the near-infrared region owing to the availability of high-power, ultrashort optical light sources, which commonly generate pulsed THz radiation with frequencies ranging from 0.2 to 4 THz (*75*, *113*–*116*), although higher frequency generation is possible, as indicated above. Pulse energies up to 1.4 mJ at 0.4 THz have been demonstrated by operating bulk PPLN crystals at cryogenic temperatures and using chirped laser pulses (*75*), with conversion efficiencies reaching up to 0.9% (*117*). The generation of continuous-wave THz radiation, tunable from 1.34 to 1.70 THz and 3.06 to 3.59 THz, has also been demonstrated using cascaded optical parametric processes in a singly resonant OPO using a bulk PPLN crystal for phase matching (*104*).

#### *Microwave frequencies*

Microwave frequencies (0.3 to 300 GHz) are used in applications such as 5G and 6G communication, radar, and radio astronomy. In recent years, "RF photonics" has become a widely used term to describe applications such as the generation of ultrastable microwave sources or the low-loss remoting of source and transmitter, which uses light to carry modulated signals to an antenna and subsequent conversion to microwaves. In the nonlinear optic context, such microwave frequencies can be generated directly through a DFG process in a whispering gallery mode resonator for the optical and microwave mode (*118*) or by using TFLN-superconductor hybrid electro-optic systems (*119*).

However, in most RF photonics applications, LN is used to translate microwave frequencies onto an optical carrier, which can then be transmitted and manipulated in the optical domain and subsequently generate microwave frequencies using a photodetector with an appropriate bandwidth. The main mechanisms of conversion from microwave to optical frequency rely on the electro-optic and acousto-optic effect in LN (see Fig. 2, B and C). Electro-optic modulators have been demonstrated in bulk crystals weakly confining waveguides (*38*), and strongly confining TFLN waveguides (*49*), with the latter being particularly attractive because of the attainable high modulation speeds and low drive voltages. The bandwidth of these electro-optic modulators can reach over 100 GHz (*49*, *64*, *120*, *121*) and even approach THz levels (*122*). Acousto-optic devices have also been demonstrated in bulk crystals, weakly confining waveguides (*123*) and strongly confining TFLN waveguides (*124*, *125*), with interaction frequencies typically ranging from MHz to GHz levels. Such acousto-optic devices are traditionally used to induce small frequency shifts, as beam deflectors, as well as moderately fast switches and power regulators (*123*–*126*). More recently, they have enabled quantum transduction for superconducting qubits (*119*, *127*), which is attributable to the small acoustic mode volume in nanophotonic resonators fabricated in TFLN.

### Future of LN technology

LN, in all three modalities (bulk LN crystals, weakly confining, and strongly confining LN waveguides), is widely used for nonlinear optic, acoustic, and electro-optic processes to generate and manipulate EM frequencies over a wide spectral range. Since LN's inception, the material and manufacturing processes have matured, resulting in mostly discrete components that perform well-defined functions. In the future, bulk LN crystal components will remain important for EM-frequency generation across the spectrum, particularly for applications that require high optical powers, such as in high-power OPOs, free-space acousto-optic and electro-optic modulators, and Q-switches in laser cavities. However, for the LN waveguide platforms, we foresee a rapid acceleration of developments across two dimensions: (i) complexity and (ii) spectral breadth (Fig. 5). Complexity will transition from millimeter-scale single components on chip to micrometer-scale nanophotonic circuits followed by complex multilayer networks in which diverse materials are heterogeneously integrated with LN and co-packaged with electronic circuits. The spectral breadth of these devices will transition from operating primarily at near-infrared frequencies to generating and manipulating EM frequencies from visible to microwave frequencies on demand.

#### *Near-term*

In the near-term (next 5 years), bulk crystals and weakly confining waveguides will remain essential platforms for the generation of EM frequencies, particularly in the near-infrared and visible frequency region because they offer mature fabrication and packaging processes. The high-power handling capability and the low interface loss of such commercially available products make them particularly attractive for serving as individual devices in system demonstrations, for example, as part of self-referencing systems for optical clocks, in which the LN components can be connected to other sophisticated photonic infrastructure. Furthermore, the low-loss interfacing of weakly confined waveguides is important for quantum optics applications, for example, for the generation of photon pairs by spontaneous parametric down-conversion as well as for frequency translation between quantum nodes and long-haul fiber networks, in addition to heterogeneous intranode conversion. Although LN is a well-studied material, more work is needed to investigate the optimization of light-induced absorption changes (photochromic effect), particularly for operations at short wavelengths (*128*).

The wider adoption of tightly confining LN waveguides is, at present, mainly hampered by two shortfalls: (i) the poorly understood uniformity, repeatability, and reliability of the commercially available starting material and (ii) the lack of low-loss interfaces to standard optical fibers. Although there has been some progress in solving the interface problem for submicron waveguides in LN (*129*, *130*), they still require specialized fibers and high-precision multistep e-beam lithography and etching, which may not be practical or economical for large-scale, fully packaged solutions.

A high-volume application, such as optical short-distance data communication, will provide the commercial means to address both the shortfalls and maturation of TFLN technologies. It will also drive the reduction of TFLN wafer and manufacturing costs as well as increase diversity in TFLN suppliers. This high-volume communication application is motivated by the ever-increasing need for data center and cloud infrastructure, which requires increased speed, reduced power consumption, and lower cost for next-generation communication systems. Indeed, TFLN is an ideal candidate because of its low drive voltage, compatibility with CMOS electronics (*49*), and high bandwidth. Long-haul telecom applications may also become commercial drivers to mature the TFLN platform because the major challenge for this application is performance, where TFLN's demonstrated data (symbol) rate of 120 gigabaud and beyond is highly attractive (*49*). These devices can be drop-in replacements for existing guided-wave LN electro-optic modulators, allowing for low threshold commercial adoption while offering performance advantages. For LiDAR applications, the recent breakthrough of Pockels cavity lasers (*131*) by integrating III-V semiconductor gain sections with TFLN-based external cavities offers unrivaled frequency modulation speed and reconfigurability to integrated lasers; injection locking of a laser diode into an external LN ring modulator can also achieve fast frequency modulation while the wavelength tuning range is limited (*132*).

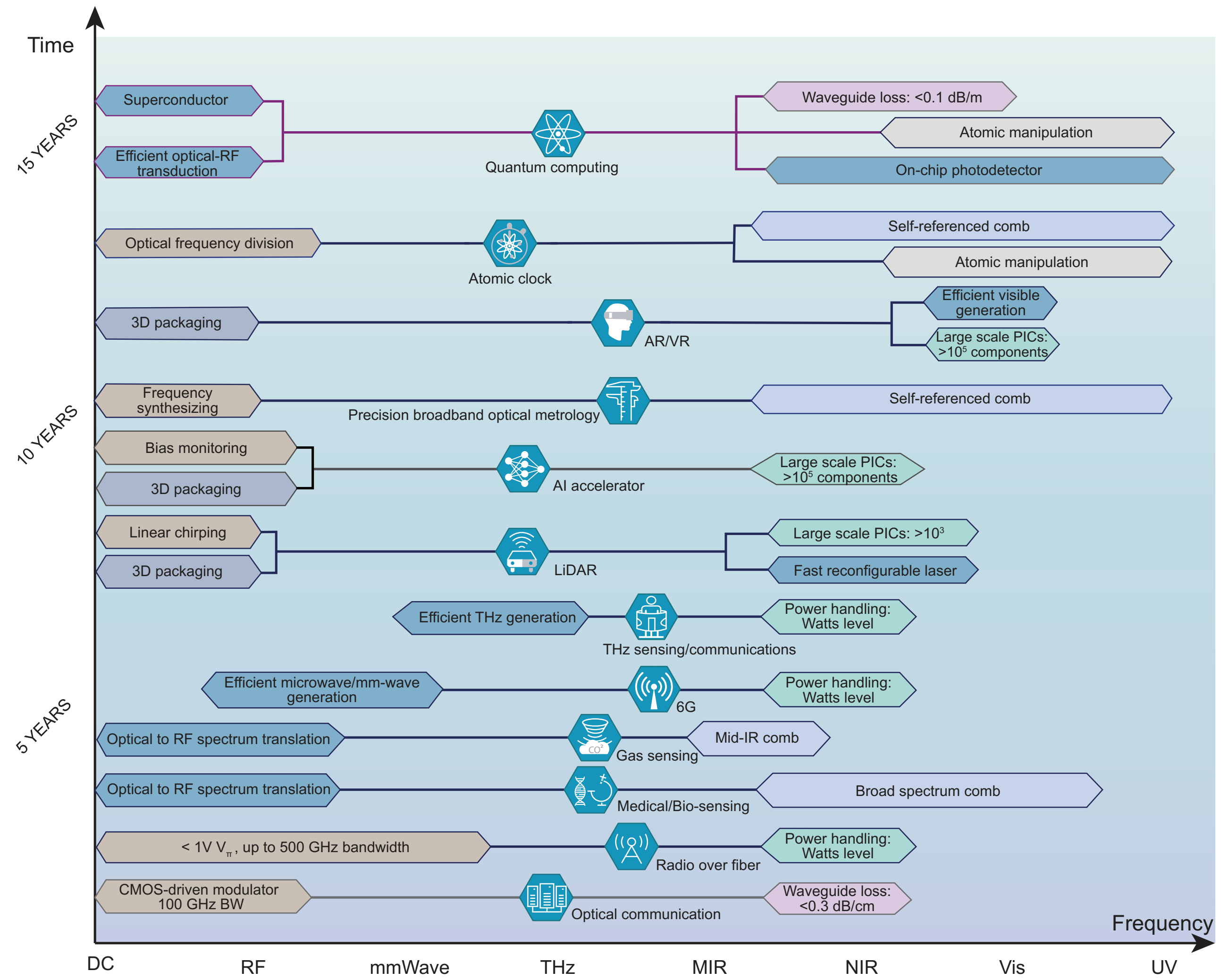


**Fig. 5. Outlook of LN photonics and its applications.** The applications are illustrated by the symbols in the center, which require the functionalities on either end of the spectrum. The continued development of quality engineering and production scalability drives the performance of photonic devices and systems, both of which jointly enable new applications. Emerging applications stimulate the improvement of material processing and high-volume device production. DC, direct current; MIR, mid-infrared; NIR, near-infrared; Vis, visible.

An alternative approach is the adiabatic frequency conversion using LN-based resonators (*133*). These approaches can potentially provide a chip-based, low-cost solution to frequency-modulated continuous-wave LiDAR. Furthermore, phase modulation with minimal intensity modulation in LN can be used to tune the emission angle of the light beam, without sensitivity degradation during the scanning. Addressing these near-term industrial applications with relatively simple, high-yield designs will help to mature the platform and achieve the statistical understanding of issues such as device yield, uniformity, repeatability, and reliability. They will also provide a better understanding of photorefractive and charging effects (e.g., bias drift in electro-optical modulators) in TFLN, which can have detrimental impacts on the performance and stability of LN PICs, particularly when their scale becomes large. We anticipate that in the next 5 years, substantial investments will be made in this space, which will build the foundation of the wide-scale adoption of tightly confining LN waveguide circuits as commercial devices.

At the same time, we foresee rapid progress in the development of TFLN at the device level for high-efficiency frequency mixing applications, such as miniaturized OPOs and optical phase arrays (OPAs) using integrated PPLN-based waveguides or microcavities, where earlier commercial adoption is feasible. For these applications, several devices can be manufactured on the same chip with parameter sweeps to account for uniformity and fabrication-tolerance issues, such that the best devices can be isolated and packaged (i.e., "hand-picked"). These devices will be of high value because they can provide ultrabroadband, ultrahigh parametric gains that reach an octave using microwatt average powers or femtojoule-level pump energies (*66*, *134*). The same approach can be used to develop widely tunable, on-chip oscillators for challenging spectral regimes, such as the visible and mid-infrared spectral ranges for addressing atomic and molecular systems used for metrology and spectroscopy, or efficient mm-wave and THz generation for wireless communication and sensing. Along this track of integrated OPOs and OPAs, squeezed-state generation for continuous-variable quantum computing, quantum random number generation, and quadratic dissipative soliton formation operating in a strongly nonlinear regime can be implemented.

One essential trend we expect to happen in the next 5 years is the development of heterogeneous integration on the TFLN platform. Based on wafer-bonding, LN waveguides will be interfaced with different materials at the wafer scale, among which the integration of III-V semiconductor materials as laser sources, amplifiers, and detectors will be crucial. Another trend that we expect will be developed is the co-packaging of photonic and electronic circuits, which is crucial for the control and monitoring of large-scale LN circuits. Although these initial efforts will be mainly at the research level, they will pave the way for future wafer-scale heterogeneous platforms with full control and monitoring and communication functionality.

### *Mid-term*

In the mid-term (5 to 10 years), we anticipate that bulk crystals and weakly confining waveguides will continue to be used as individual components for low-volume, price-sensitive visible to mid-infrared frequency applications. Emerging applications such as 6G or THz sensing will benefit from the high power-handling capability of these devices for efficient microwave and THz generation. However, the relatively high material losses at the THz spectral region (*135*, *136*) can be detrimental for device performance and require the generation of the THz radiation near the LN-air interface (*75*, *137*).

In parallel, we predict that improved low-loss optical interfaces to submicron waveguides and fabrication processes that are developed for high-volume data communication applications will result in an increased uptake of tightly confining TFLN waveguide circuits for near-infrared frequency applications. One of the challenges to be overcome in the mid-term is the reproducibility of nanophotonic components. For example, networks of virtually identical degenerate OPOs would be highly valuable for wavelength agile information processing. However, the high sensitivity of the nonlinear function of OPOs to the precise dispersion throughout the device imposes stringent requirements on the fabrication tolerance (waveguide widths and etch depth), wafer uniformity (film thickness, both within a single wafer as well from wafer-to-wafer) and also defect control. Active tuning and post-processing might hold solutions to these challenges. Hence, similar to silicon photonic circuits, one could rely on thermal heaters for tuning, which is not attractive for energy efficiency reasons, or the integration of advanced refractive index tunable materials (*138*). Where available, noncritical designs should be implemented to increase dimensional tolerances (*139*, *140*). This may be achievable when expanding the design space by considering sophisticated cladding structures, such as multilayer stacks.

Along with the improved fabrication processes and reproducibility of nanophotonic components, we anticipate that data communication applications will push forward the co-packaging of photonic and electronic circuits and the heterogeneous integration of active materials for near-infrared light sources and detectors (*57*), thereby transferring the fabrication processes that have been developed for silicon photonic circuits (*141*) to the TFLN platform. The integration of lasers and detectors will also be highly appealing to numerous applications that demand large-scale, fully integrated PICs, such as analog microwave photonics, LiDAR, and artificial intelligence (AI). Although at this stage the scalability of OPAs or optical neural networks (ONNs) might not be as vast as that available in silicon photonics, these applications will benefit immensely from the TFLN technology because of the substantially reduced drive voltage, increased bandwidth, and low insertion loss. Additionally, it is plausible to anticipate that complex and high-performance analog systems, including 6G mm-wave systems, RF spectrum analyzers, and photonic analog-to-digital converters, will be realized on TFLN. Importantly, these applications can benefit from the reduced cost by using the matured, near-infrared components to make the dream of the wide adoption of photonic-based, wideband-RF systems a reality.

Additionally, we envision a more complex system that operates from microwave wavelengths down to visible wavelengths and is enabled by further integration of electro-optic, acousto-optic, and all-optical signal-processing components. One of the foreseeable areas where LN can make a revolutionary impact is in OFC technology. As a material with both second-order and Kerr nonlinearity along with high-bandwidth modulators, LN is extremely suitable for realizing integrated self-referenced OFCs on a single nanophotonic platform with laser sources, amplifiers, and high-speed photodetectors that are heterogeneously integrated, where ultraefficient nonlinear broadening and SHG are readily accessible functions. In addition, the realization of cascading a series of low–switching voltage, high-bandwidth electro-optic modulators would promise, among many other applications, frequency-agile, electro-optic frequency combs with a considerable versatility in center wavelengths and repetition rates as well as direct synthesis of femtosecond-class pulse sources without mode locking (*142*). Such sources naturally operate at repetition rates that are compatible with on-chip resonators and thus open a wide range of opportunities in highly efficient nonlinear frequency conversion using pulsed pumping schemes. Other mid-term applications might involve dynamic beamforming based on electro- or acousto-optic devices, which is essential for LiDAR, augmented and virtual reality displays, and trapped-ion quantum computing systems. The major challenge in the mid-term is to establish innovative system architectures that can use different light-matter interactions (between microwave, mechanical, and optical subcomponents) without paying a substantial price in performance and manufacturing complexity.

### *Long-term*

In the long-term (10 years and beyond), TFLN will be based on a large-scale (beyond 200-mm diameter wafer) foundry process with diverse heterogeneously integrated materials and co-packaged electronic circuits. Such a platform will be an excellent choice for scaling up optical networking schemes in which large arrays of classical or quantum light sources or processing units need to be coupled, often in a programmable way. This will enable fundamentally innovative applications such as fully integrated LiDAR and ONNs, quantum computing, fully integrated frequency synthesizers, massive RF signal processing networks, and advanced sensors. For example, photonic AI accelerators require an array of low–energy cost electro-optic modulators and nonlinear photonic activation components. In addition to neural networks, other photonic architectures for optical computing such as coherent Ising machines also demand a large number of photonic-based artificial spins connected by a reconfigurable all-to-all coupling matrix. Regardless of whether a time or spatially multiplexed approach is used, TFLN devices are critical to realizing photonic spins based on degenerate OPOs as well as spin-spin coupling based on delay lines with amplitude and phase modulators or a Mach-Zehnder interferometer mesh. Topological studies in synthetic dimensions could also be interesting in such coupled resonator networks.

A grand challenge in quantum engineering is to achieve extreme optical nonlinearity (ideally at the single-photon level) where both improvement of material processing and nanoengineering are required. We do see benefits from gradual improvements in optical nonlinearity using LN in future quantum PICs. This will benefit quantum photonic systems in which spatially multiplexed spontaneous parametric down-conversion sources with fast feedback optical switches are required for the implementation of near-deterministic single-photon sources or large scale continuous-variable computation in which high-quality squeezing states are required. Regarding quantum communication networks and all-optical signal processing, we envision that spectrotemporal shaping and quantum transduction techniques will have to be used to overcome the inhomogeneity of quantum emitters or to bridge the spectral difference between heterogeneous quantum systems. Furthermore, LN's fast modulation capability with low loss based on the electro-optic effect will be essential in almost all the quantum systems to increase processing speed and reduce system losses.

Fortunately, LN is an all-around high-performance optical material that is able to generate and manipulate EM frequencies on demand over a spectral range that covers nearly five orders of magnitude with a proven history of reliability and an ever-growing diverse portfolio of near- to long-term applications based on its nanophotonic platform. It is important to note that we anticipate that PICs that make use of TFLN will require heterogeneous integration to enable the integration of the attractive material properties of LN with efficient light sources and detectors. This may be realized by heterogeneously integrating such PIC elements on the TFLN waveguide platform (*57*) or by integrating thin films of LN onto other PIC material platforms (*143*). Independent of its modality (bulk crystal, weakly confined, or tightly confined waveguides) or, indeed, integration method, LN is in a great position to overcome the outlined challenges to become the material platform of choice for unlocking the EM spectrum and to continue to revolutionize optical science for years to come.

#### REFERENCES AND NOTES


1. P. Marin-Palomo *et al*., Microresonator-based solitons for massively parallel coherent optical communications. *Nature* **546**, 274–279 (2017). doi: 10.1038/nature22387; pmid: 28593968
2. B. Corcoran *et al*., Ultra-dense optical data transmission over standard fibre with a single chip source. *Nat. Commun.* **11**, 2568 (2020). doi: 10.1038/s41467-020-16265-x; pmid: 32444605
3. T. W. Hänsch, Nobel lecture: Passion for precision. *Rev. Mod. Phys.* **78**, 1297–1309 (2006). doi: 10.1103/RevModPhys.78.1297
4. J. L. Hall, Nobel lecture: Defining and measuring optical frequencies. *Rev. Mod. Phys.* **78**, 1279–1295 (2006). doi: 10.1103/RevModPhys.78.1279; pmid: 17086589
5. H. R. Telle *et al*., Carrier-envelope offset phase control: A novel concept for absolute optical frequency measurement and ultrashort pulse generation. *Appl. Phys. B* **69**, 327–332 (1999). doi: 10.1007/s003400050813
6. R. Prevedel, A. Diz-Muñoz, G. Ruocco, G. Antonacci, Brillouin microscopy: An emerging tool for mechanobiology. *Nat. Methods* **16**, 969–977 (2019). doi: 10.1038/s41592-019-0543-3; pmid: 31548707
7. J. G. Fujimoto, Optical coherence tomography for ultrahigh resolution in vivo imaging. *Nat. Biotechnol.* **21**, 1361–1367 (2003). doi: 10.1038/nbt892; pmid: 14595364
8. U. Morgner *et al*., Spectroscopic optical coherence tomography. *Opt. Lett.* **25**, 111–113 (2000). doi: 10.1364/OL.25.000111; pmid: 18059799
9. T. D. Ladd *et al*., Quantum computers. *Nature* **464**, 45–53 (2010). doi: 10.1038/nature08812; pmid: 20203602
10. S. Wehner, D. Elkouss, R. Hanson, Quantum internet: A vision for the road ahead. *Science* **362**, eaam9288 (2018). doi: 10.1126/science.aam9288; pmid: 30337383
11. M. Manzo, F. Laurell, V. Pasiskevicius, K. Gallo, "Lithium niobate: The silicon of photonics!" in *Nano-Optics for Enhancing Light-Matter Interactions on a Molecular Scale*, B. Di Bartolo, J. Collins, Eds. (NATO Science for Peace and Security Series B: Physics and Biophysics, Springer, 2013), pp. 421–422.
12. B. T. Matthias, J. P. Remeika, Ferroelectricity in the ilmenite structure. *Phys. Rev.* **76**, 1886–1887 (1949). doi: 10.1103/PhysRev.76.1886.2
13. G. E. Peterson, A. A. Ballman, P. V. Lenzo, P. M. Bridenbaugh, Electro-optic properties of LiNbO3. *Appl. Phys. Lett.* **5**, 62–64 (1964). doi: 10.1063/1.1754053
14. R. G. Smith, K. Nassau, M. F. Galvin, Efficient continuous optical second-harmonic generation. *Appl. Phys. Lett.* **7**, 256–258 (1965). doi: 10.1063/1.1754246
15. K. Nassau, H. J. Levinstein, G. M. Loiacono, Ferroelectric lithium niobate. 1. Growth, domain structure, dislocations and etching. *J. Phys. Chem. Solids* **27**, 983–988 (1966). doi: 10.1016/0022-3697(66)90070-9
16. K. Nassau, H. J. Levinstein, G. M. Loiacono, Ferroelectric lithium niobate. 2. Preparation of single domain crystals. *J. Phys. Chem. Solids* **27**, 989–996 (1966). doi: 10.1016/0022-3697(66)90071-0
17. M. Yamada, N. Nada, M. Saitoh, K. Watanabe, First-order quasi-phase matched LiNbO3 waveguide periodically poled by applying an external field for efficient blue second-harmonic generation. *Appl. Phys. Lett.* **62**, 435–436 (1993). doi: 10.1063/1.108925
18. L. Huang, N. A. F. Jaeger, Discussion of domain inversion in LiNbO3. *Appl. Phys. Lett.* **65**, 1763–1765 (1994). doi: 10.1063/1.112911
19. A. Ashkin *et al*., Optically-induced refractive index inhomogeneities in $LiNbO_3$ AND $LiTaO_3$. *Appl. Phys. Lett.* **9**, 72–74 (1966). doi: 10.1063/1.1754607
20. F. H. Mok, M. C. Tackitt, H. M. Stoll, Storage of 500 high-resolution holograms in a $LiNbO_3$ crystal. *Opt. Lett.* **16**, 605–607 (1991). doi: 10.1364/OL.16.000605; pmid: 19774013
21. C. R. Phillips, J. S. Pelc, M. M. Fejer, Continuous wave monolithic quasi-phase-matched optical parametric oscillator in periodically poled lithium niobate. *Opt. Lett.* **36**, 2973–2975 (2011). doi: 10.1364/OL.36.002973; pmid: 21808376
22. T. Beckmann *et al*., Highly tunable low-threshold optical parametric oscillation in radially poled whispering gallery resonators. *Phys. Rev. Lett.* **106**, 143903 (2011). doi: 10.1103/PhysRevLett.106.143903; pmid: 21561193
23. S. Schiller, R. L. Byer, Quadruply resonant optical parametric oscillation in a monolithic total-internal-reflection resonator. *J. Opt. Soc. Am. B* **10**, 1696 (1993). doi: 10.1364/JOSAB.10.001696
24. V. S. Ilchenko, A. B. Matsko, A. A. Savchenkov, L. Maleki, "High-efficiency microwave and millimeter-wave electro-optical modulation with whispering-gallery resonators" in *Laser Resonators and Beam Control V*, vol. 4629 of *SPIE Proceedings*, A. V. Kudryashov, Ed. (SPIE, 2002), pp. 158–163.
25. V. S. Ilchenko, A. A. Savchenkov, A. B. Matsko, L. Maleki, Nonlinear optics and crystalline whispering gallery mode cavities. *Phys. Rev. Lett.* **92**, 043903 (2004). doi: 10.1103/PhysRevLett.92.043903; pmid: 14995375
26. D. Wei *et al*., Experimental demonstration of a three-dimensional lithium niobate nonlinear photonic crystal. *Nat. Photonics* **12**, 596–600 (2018). doi: 10.1038/s41566-018-0240-2
27. L. E. Myers *et al*., Quasi-phase-matched 1.064-microm-pumped optical parametric oscillator in bulk periodically poled $LiNbO_3$. *Opt. Lett.* **20**, 52–54 (1995). doi: 10.1364/OL.20.000052; pmid: 19855794
28. U. Strößner *et al*., Single-frequency continuous-wave optical parametric oscillator system with an ultrawide tuning range of 550 to 2830 nm. *J. Opt. Soc. Am. B* **19**, 1419 (2002). doi: 10.1364/JOSAB.19.001419
29. I. P. Kaminow, J. R. Carruthers, Optical waveguiding layers in $LiNbO_3$ and $LiTaO_3$. *Appl. Phys. Lett.* **22**, 326–328 (1973). doi: 10.1063/1.1654657
30. R. V. Schmidt, I. P. Kaminow, Metal-diffused optical waveguides in $LiNbO_3$. *Appl. Phys. Lett.* **25**, 458–460 (1974). doi: 10.1063/1.1655547
31. J. L. Jackel, C. E. Rice, J. J. Veselka, Proton exchange for high-index waveguides in $LiNbO_3$. *Appl. Phys. Lett.* **41**, 607–608 (1982). doi: 10.1063/1.93615
32. L. Gui, B. Xu, T. C. Chong, Microstructure in lithium niobate by use of focused femtosecond laser pulses. *IEEE Photonics Technol. Lett.* **16**, 1337–1339 (2004). doi: 10.1109/LPT.2004.826112
33. G. Bava, I. Montrosset, W. Sohler, H. Suche, Numerical modeling of Ti:$LiNbO_3$ integrated optical parametric oscillators. *IEEE J. Quantum Electron.* **23**, 42–51 (1987). doi: 10.1109/JQE.1987.1073210
34. Y. N. Korkishko, V. A. Fedorov, Relationship between refractive indices and hydrogen concentration in proton exchanged $LiNbO_3$ waveguides. *J. Appl. Phys.* **82**, 1010–1017 (1997). doi: 10.1063/1.365864
35. J. Webjorn, F. Laurell, G. Arvidsson, Fabrication of periodically domain-inverted channel waveguides in lithium niobate for second harmonic generation. *J. Lightwave Technol.* **7**, 1597–1600 (1989). doi: 10.1109/50.39103
36. E. J. Lim, M. M. Fejer, R. L. Byer, Second-harmonic generation of green light in periodically poled planar lithium niobate waveguide. *Electron. Lett.* **25**, 174 (1989). doi: 10.1049/el:19890127
37. R. Brinkmann, W. Sohler, H. Suche, Continuous-wave erbium-diffused $LiNbO_3$ waveguide laser. *Electron. Lett.* **27**, 415 (1991). doi: 10.1049/el:19910263
38. E. L. Wooten *et al*., Review of lithium niobate modulators for fiber-optic communications systems. *IEEE J. Sel. Top. Quantum Electron.* **6**, 69–82 (2000). doi: 10.1109/2944.826874
39. C. Langrock *et al*., Highly efficient single-photon detection at communication wavelengths by use of upconversion in reverse-proton-exchanged periodically poled $LiNbO_3$ waveguides. *Opt. Lett.* **30**, 1725–1727 (2005). doi: 10.1364/OL.30.001725; pmid: 16075551
40. H. Jin *et al*., On-chip generation and manipulation of entangled photons based on reconfigurable lithium-niobate waveguide circuits. *Phys. Rev. Lett.* **113**, 103601 (2014). doi: 10.1103/PhysRevLett.113.103601; pmid: 25238358
41. J. Gil-Lopez *et al*., Improved non-linear devices for quantum applications. *New J. Phys.* **23**, 063082 (2021). doi: 10.1088/1367-2630/ac09fd
42. C. Langrock, S. Kumar, J. E. McGeehan, A. E. Willner, M. M. Fejer, All-optical signal processing using /spl chi//sup (2)/ nonlinearities in guided-wave devices. *J. Lightwave Technol.* **24**, 2579–2592 (2006). doi: 10.1109/JLT.2006.874605
43. P. Rabiei, P. Gunter, Optical and electro-optical properties of submicrometer lithium niobate slab waveguides prepared by crystal ion slicing and wafer bonding. *Appl. Phys. Lett.* **85**, 4603–4605 (2004). doi: 10.1063/1.1819527
44. H. Hu, R. Ricken, W. Sohler, Lithium niobate photonic wires. *Opt. Express* **17**, 24261–24268 (2009). doi: 10.1364/OE.17.024261; pmid: 20052137
45. L. Chang *et al*., Thin film wavelength converters for photonic integrated circuits. *Optica* **3**, 531 (2016). doi: 10.1364/OPTICA.3.000531
46. M. Zhang, C. Wang, R. Cheng, A. Shams-Ansari, M. Lončar, Monolithic ultra-high-Q lithium niobate microring resonator. *Optica* **4**, 1536 (2017). doi: 10.1364/OPTICA.4.001536
47. J. Lu *et al*., Periodically poled thin-film lithium niobate microring resonators with a second-harmonic generation efficiency of 250,000%/W. *Optica* **6**, 1455 (2019). doi: 10.1364/OPTICA.6.001455
48. R. Wolf *et al*., Quasi-phase-matched nonlinear optical frequency conversion in on-chip whispering galleries. *Optica* **5**, 872 (2018). doi: 10.1364/OPTICA.5.000872
49. C. Wang *et al*., Integrated lithium niobate electro-optic modulators operating at CMOS-compatible voltages. *Nature* **562**, 101–104 (2018). doi: 10.1038/s41586-018-0551-y; pmid: 30250251
50. K. Aoki *et al*., Single-drive X-cut thin-sheet $LiNbO_3$ optical modulator with chirp adjusted using asymmetric CPW electrode. *J. Lightwave Technol.* **24**, 2233–2237 (2006). doi: 10.1109/JLT.2006.872303
51. C. Wang *et al*., Monolithic lithium niobate photonic circuits for Kerr frequency comb generation and modulation. *Nat. Commun.* **10**, 978 (2019). doi: 10.1038/s41467-019-08969-6; pmid: 30816151
52. Y. He *et al*., Self-starting bi-chromatic $LiNbO_3$ soliton microcomb. *Optica* **6**, 1138 (2019). doi: 10.1364/OPTICA.6.001138
53. M. Zhang *et al*., Broadband electro-optic frequency comb generation in a lithium niobate microring resonator. *Nature* **568**, 373–377 (2019). doi: 10.1038/s41586-019-1008-7; pmid: 30858615
54. X. Liu *et al*., Tunable single-mode laser on thin film lithium niobate. *Opt. Lett.* **46**, 5505–5508 (2021). doi: 10.1364/OL.441167; pmid: 34724512
55. Y. Liu *et al*., On-chip erbium-doped lithium niobate microcavity laser. *Sci. China Phys. Mech. Astron.* **64**, 234262 (2021). doi: 10.1007/s11433-020-1625-9
56. K. Luke *et al*., Wafer-scale low-loss lithium niobate photonic integrated circuits. *Opt. Express* **28**, 24452–24458 (2020). doi: 10.1364/OE.401959; pmid: 32906986
57. C. Op de Beeck *et al*., III/V-on-lithium niobate amplifiers and lasers. *Optica* **8**, 1288 (2021).
58. T. Komljenovic *et al*., Photonic integrated circuits using heterogeneous integration on silicon. *Proc. IEEE Inst. Electr. Electron. Eng.* **106**, 2246–2257 (2018).
59. M. Jankowski *et al*., Ultrabroadband nonlinear optics in nanophotonic periodically poled lithium niobate waveguides. *Optica* **7**, 40 (2020). doi: 10.1364/OPTICA.7.000040

60. D. Zhu *et al*., Integrated photonics on thin-film lithium niobate. *Adv. Opt. Photonics* **13**, 242 (2021). doi: 10.1364/AOP.411024
61. L. Arizmendi, Photonic applications of lithium niobate crystals. *Phys. Status Solidi, A Appl. Res.* **201**, 253–283 (2004). doi: 10.1002/pssa.200303911
62. G. Chen *et al*., Advances in lithium niobate photonics: Development status and perspectives. *Adv. Photonics* **4**, (2022). doi: 10.1117/1.AP.4.3.034003
63. M. G. Vazimali, S. Fathpour, Applications of thin-film lithium niobate in nonlinear integrated photonics. *Adv. Photonics* **4**, (2022). doi: 10.1117/1.AP.4.3.034001
64. M. Zhang, C. Wang, P. Kharel, D. Zhu, M. Lončar, Integrated lithium niobate electro-optic modulators: When performance meets scalability. *Optica* **8**, 652 (2021). doi: 10.1364/OPTICA.415762
65. Y. Qi, Y. Li, Integrated lithium niobate photonics. *Nanophotonics* **9**, 1287–1320 (2020). doi: 10.1515/nanoph-2020-0013
66. L. Ledezma *et al*., Intense optical parametric amplification in dispersion-engineered nanophotonic lithium niobate waveguides. *Optica* **9**, 303 (2022). doi: 10.1364/OPTICA.442332
67. C. Wang *et al*., Second harmonic generation in nano-structured thin-film lithium niobate waveguides. *Opt. Express* **25**, 6963–6973 (2017). doi: 10.1364/OE.25.006963; pmid: 28381038
68. V. Y. Shur, A. R. Akhmatkhanov, I. S. Baturin, Micro- and nano-domain engineering in lithium niobate. *Appl. Phys. Rev.* **2**, 040604 (2015). doi: 10.1063/1.4928591
69. G. Rosenman, P. Urenski, A. Agronin, Y. Rosenwaks, M. Molotskii, Submicron ferroelectric domain structures tailored by high-voltage scanning probe microscopy. *Appl. Phys. Lett.* **82**, 103–105 (2003). doi: 10.1063/1.1534410
70. G. Imeshev *et al*., Engineerable femtosecond pulse shaping by second-harmonic generation with Fourier synthetic quasi-phase-matching gratings. *Opt. Lett.* **23**, 864–866 (1998). doi: 10.1364/OL.23.000864; pmid: 18087367
71. M. Asobe *et al*., Engineered quasi-phase matching device for unequally spaced multiple wavelength generation and its application to midinfrared gas sensing. *IEEE J. Quantum Electron.* **46**, 447–453 (2010). doi: 10.1109/JQE.2009.2032366
72. G. Imeshev *et al*., Ultrashort-pulse second-harmonic generation with longitudinally nonuniform quasi-phase-matching gratings: Pulse compression and shaping. *J. Opt. Soc. Am. B* **17**, 304 (2000). doi: 10.1364/JOSAB.17.000304
73. C. J. Xin *et al*., Spectrally separable photon-pair generation in dispersion engineered thin-film lithium niobate. *Opt. Lett.* **47**, 2830–2833 (2022). doi: 10.1364/OL.456873; pmid: 35648941
74. N. Leindecker, A. Marandi, R. L. Byer, K. L. Vodopyanov, Broadband degenerate OPO for mid-infrared frequency comb generation. *Opt. Express* **19**, 6296–6302 (2011). doi: 10.1364/OE.19.006296; pmid: 21451655
75. B. Zhang *et al*., 1.4-mJ high energy terahertz radiation from lithium niobates. *Laser Photonics Rev.* **15**, 2000295 (2021). doi: 10.1002/lpor.202000295
76. M. Yu, B. Desiatov, Y. Okawachi, A. L. Gaeta, M. Lončar, Coherent two-octave-spanning supercontinuum generation in lithium-niobate waveguides. *Opt. Lett.* **44**, 1222–1225 (2019). doi: 10.1364/OL.44.001222; pmid: 30821753
77. J. Rutledge *et al*., Broadband ultraviolet-visible frequency combs from cascaded high-harmonic generation in quasi-phase-matched waveguides. *J. Opt. Soc. Am. B* **38**, 2252 (2021). doi: 10.1364/JOSAB.427086
78. C. Nico, T. Monteiro, M. P. F. Graça, Niobium oxides and niobates physical properties: Review and prospects. *Prog. Mater. Sci.* **80**, 1–37 (2016). doi: 10.1016/j.pmatsci.2016.02.001
79. M. Hu *et al*., Virtual reality: A survey of enabling technologies and its applications in IoT. *J. Netw. Comput. Appl.* **178**, 102970 (2021). doi: 10.1016/j.jnca.2020.102970
80. N. Chauhan *et al*., Ultra-low loss visible light waveguides for integrated atomic, molecular, and quantum photonics. *Opt. Express* **30**, 6960–6969 (2022). doi: 10.1364/OE.448938; pmid: 35299469
81. A. Al Sayem *et al*., Efficient and tunable blue light generation using lithium niobate nonlinear photonics. *Appl. Phys. Lett.* **119**, 231104 (2021). doi: 10.1063/5.0071769
82. J. Capmany, Simultaneous generation of red, green, and blue continuous-wave laser radiation in Nd3 -doped aperiodically poled lithium niobate. *Appl. Phys. Lett.* **78**, 144–146 (2001). doi: 10.1063/1.1338495
83. L. Carletti *et al*., Steering and encoding the polarization of the second harmonic in the visible with a monolithic $LiNbO_3$ metasurface. *ACS Photonics* **8**, 731–737 (2021). doi: 10.1021/acsphotonics.1c00026; pmid: 33842671
84. G. D. Miller, R. G. Batchko, M. M. Fejer, R. L. Byer, "Visible quasi-phase-matched harmonic generation by electric-field-poled lithium niobate" in *Nonlinear Frequency Generation and Conversion*, vol. 2700 of *SPIE Proceedings*, M. C. Gupta, W. J. Kozlovsky, D. C. MacPherson, Eds. (SPIE, 1996).
85. S. Sinha, C. Langrock, M. J. F. Digonnet, M. M. Fejer, R. L. Byer, Efficient yellow-light generation by frequency doubling a narrow-linewidth 1150 nm ytterbium fiber oscillator. *Opt. Lett.* **31**, 347–349 (2006). doi: 10.1364/OL.31.000347; pmid: 16480204
86. M. Reig Escalé, F. Kaufmann, H. Jiang, D. Pohl, R. Grange, Generation of 280 THz-spanning near-ultraviolet light in lithium niobate-on-insulator waveguides with sub-100 pJ pulses. *APL Photonics* **5**, 121301 (2020). doi: 10.1063/5.0028776
87. R. Normandin, G. I. Stegeman, Nondegenerate four-wave mixing in integrated optics. *Opt. Lett.* **4**, 58 (1979). doi: 10.1364/OL.4.000058; pmid: 19684783
88. S. Liu *et al*., Effective four-wave mixing in the lithium niobate on insulator microdisk by cascading quadratic processes. *Opt. Lett.* **44**, 1456–1459 (2019). doi: 10.1364/OL.44.001456; pmid: 30874675
89. D. Marpaung, J. Yao, J. Capmany, Integrated microwave photonics. *Nat. Photonics* **13**, 80–90 (2019). doi: 10.1038/s41566-018-0310-5
90. J. Riemensberger *et al*., "Massively parallel coherent LiDAR using dissipative Kerr solitons" in *Conference on Lasers and Electro-Optics*, OSA Technical Digest (Optica Publishing Group, 2020), paper SM2N.2.doi: 10.1364/CLEO_SI.2020.SM2N.2
91. M. Yu *et al*., Raman lasing and soliton mode-locking in lithium niobate microresonators. *Light Sci. Appl.* **9**, 9 (2020). doi: 10.1038/s41377-020-0246-7;pmid: 31969982
92. K. C. Burr, C. L. Tang, M. A. Arbore, M. M. Fejer, High-repetition-rate femtosecond optical parametric oscillator based on periodically poled lithium niobate. *Appl. Phys. Lett.* **70**, 3341–3343 (1997). doi: 10.1063/1.119164
93. P.-K. Chen, I. Briggs, S. Hou, L. Fan, Ultra-broadband quadrature squeezing with thin-film lithium niobate nanophotonics. *Opt. Lett.* **47**, 1506–1509 (2022). doi: 10.1364/OL.447695; pmid: 35290350
94. V. D. Vaidya *et al*., Broadband quadrature-squeezed vacuum and nonclassical photon number correlations from a nanophotonic device. *Sci. Adv.* **6**, eaba9186 (2020). doi: 10.1126/sciadv.aba9186; pmid: 32967824
95. T. Kashiwazaki *et al*., Continuous-wave 6-dB-squeezed light with 2.5-THz-bandwidth from single-mode PPLN waveguide. *APL Photonics* **5**, 036104 (2020). doi: 10.1063/1.5142437
96. Z. Gong, X. Liu, Y. Xu, H. X. Tang, Near-octave lithium niobate soliton microcomb. *Optica* **7**, 1275 (2020). doi: 10.1364/OPTICA.400994
97. R. Wolf, I. Breunig, H. Zappe, K. Buse, Cascaded second-order optical nonlinearities in on-chip micro rings. *Opt. Express* **25**, 29927–29933 (2017). doi: 10.1364/OE.25.029927; pmid: 29221028
98. C. R. Phillips *et al*., Supercontinuum generation in quasi-phase-matched $LiNbO_3$ waveguide pumped by a Tm-doped fiber laser system. *Opt. Lett.* **36**, 3912–3914 (2011). doi: 10.1364/OL.36.003912; pmid: 21964139
99. A. Rueda, F. Sedlmeir, M. Kumari, G. Leuchs, H. G. L. Schwefel, Resonant electro-optic frequency comb. *Nature* **568**, 378–381 (2019). doi: 10.1038/s41586-019-1110-x; pmid: 30996319
100. A. J. Metcalf, V. Torres-Company, D. E. Leaird, A. M. Weiner, High-power broadly tunable electrooptic frequency comb generator. *IEEE J. Sel. Top. Quantum Electron.* **19**, 231–236 (2013). doi: 10.1109/JSTQE.2013.2268384
101. M. Lončar *et al*., Integrated high-efficiency and broadband electro-optic frequency comb generators. *Nat. Photon.* **16**, 679–685 (2022). doi: 10.1109/JSTQE.2013.2268384
102. M. Leidinger *et al*., Comparative study on three highly sensitive absorption measurement techniques characterizing lithium niobate over its entire transparent spectral range. *Opt. Express* **23**, 21690–21705 (2015). doi: 10.1364/OE.23.021690; pmid: 26368148
103. T. Shimanouchi, *Tables of Molecular Vibrational Frequencies, Consolidated Volume I* (NSRDS-NBS 39, Secretary of Commerce, 1972).
104. J. Kiessling, R. Sowade, I. Breunig, K. Buse, V. Dierolf, Cascaded optical parametric oscillations generating tunable terahertz waves in periodically poled lithium niobate crystals. *Opt. Express* **17**, 87–91 (2009). doi: 10.1364/OE.17.000087; pmid: 19129876
105. I. Galli *et al*., Ti:sapphire laser intracavity difference-frequency generation of 30 mW cw radiation around 4.5 μm. *Opt. Lett.* **35**, 3616–3618 (2010). doi: 10.1364/OL.35.003616; pmid: 21042368
106. T. Beddard, M. Ebrahimzadeh, T. D. Reid, W. Sibbett, Five-optical-cycle pulse generation in the mid infrared from an optical parametric oscillator based on aperiodically poled lithium niobate. *Opt. Lett.* **25**, 1052–1054 (2000). doi: 10.1364/OL.25.001052; pmid: 18064270
107. D. Richter *et al*., High-power, tunable difference frequency generation source for absorption spectroscopy based on a ridge waveguide periodically poled lithium niobate crystal. *Opt. Express* **15**, 564–571 (2007). doi: 10.1364/OE.15.000564; pmid: 19532275
108. K.-D. F. Büchter, H. Herrmann, C. Langrock, M. M. Fejer, W. Sohler, All-optical Ti:PPLN wavelength conversion modules for free-space optical transmission links in the mid-infrared. *Opt. Lett.* **34**, 470–472 (2009). doi: 10.1364/OL.34.000470; pmid: 19373344
109. J. Mishra *et al*., Mid-infrared nonlinear optics in thin-film lithium niobate on sapphire. *OSA Nonlinear Optics* **2021**, NW3A.5 (2021). doi: 10.1364/NLO.2021.NW3A.5
110. Z. Gong *et al*., Soliton microcomb generation at 2 μm in z-cut lithium niobate microring resonators. *Opt. Lett.* **44**, 3182–3185 (2019). doi: 10.1364/OL.44.003182; pmid: 31199411
111. A. S. Kowligy *et al*., Mid-infrared frequency comb generation via cascaded quadratic nonlinearities in quasi-phase-matched waveguides. *Opt. Lett.* **43**, 1678–1681 (2018). doi: 10.1364/OL.43.001678; pmid: 29652338
112. X. Liu *et al*., Sub-terahertz bandwidth capactively-loaded thin-film lithium niobate electro-optic modulators based on an undercut structure. *Opt. Express* **29**, 41798 (2021). doi: 10.1364/OE.442091
113. Q. Tian *et al*., Efficient generation of a high-field terahertz pulse train in bulk lithium niobate crystals by optical rectification. *Opt. Express* **29**, 9624–9634 (2021). doi: 10.1364/OE.419709; pmid: 33820386
114. W. R. Huang *et al*., Highly efficient terahertz pulse generation by optical rectification in stoichiometric and cryo-cooled congruent lithium niobate. *J. Mod. Opt.* **62**, 1486–1493 (2015). doi: 10.1080/09500340.2013.868547
115. S.-W. Huang *et al*., High conversion efficiency, high energy terahertz pulses by optical rectification in cryogenically cooled lithium niobate. *Opt. Lett.* **38**, 796–798 (2013). doi: 10.1364/OL.38.000796; pmid: 23455302
116. J. A. L'huillier *et al*., Generation of THz radiation using bulk, periodically and aperiodically poled lithium niobate—Part 2: Experiments. *Appl. Phys. B* **86**, 197–208 (2007). doi: 10.1007/s00340-006-2528-z
117. H. T. Olgun *et al*., Highly efficient generation of narrowband terahertz radiation driven by a two-spectral-line laser in PPLN. *Opt. Lett.* **47**, 2374–2377 (2022). doi: 10.1364/OL.448457; pmid: 35561354
118. A. Rueda *et al*., Efficient microwave to optical photon conversion: An electro-optical realization. *Optica* **3**, 597 (2016). doi: 10.1364/OPTICA.3.000597
119. Y. Xu *et al*., Bidirectional interconversion of microwave and light with thin-film lithium niobate. *Nat. Commun.* **12**, 4453 (2021). doi: 10.1038/s41467-021-24809-y; pmid: 34294711
120. P. O. Weigel *et al*., Bonded thin film lithium niobate modulator on a silicon photonics platform exceeding 100 GHz 3-dB electrical modulation bandwidth. *Opt. Express* **26**, 23728–23739 (2018). doi: 10.1364/OE.26.023728; pmid: 30184869
121. F. Yang *et al*., Monolithic thin film lithium niobate electro-optic modulator with over 110 GHz bandwidth. *Chin. Opt. Lett.* **20**, 022502 (2022). doi: 10.3788/COL202220.022502
122. A. J. Mercante *et al*., Thin film lithium niobate electro-optic modulator with terahertz operating bandwidth. *Opt. Express* **26**, 14810–14816 (2018). doi: 10.1364/OE.26.014810; pmid: 29877417
123. Z. Y. Cheng, C. S. Tsai, Baseband integrated acousto-optic frequency shifter. *Appl. Phys. Lett.* **60**, 12–14 (1992). doi: 10.1063/1.107347
124. L. Shao *et al*., Integrated microwave acousto-optic frequency shifter on thin-film lithium niobate. *Opt. Express* **28**,

23728–23738 (2020). doi: 10.1364/OE.397138; pmid: 32752365
125. L. Shao *et al*., Microwave-to-optical conversion using lithium niobate thin-film acoustic resonators. *Optica* **6**, 1498 (2019). doi: 10.1364/OPTICA.6.001498
126. C. J. Sarabalis, T. P. McKenna, R. N. Patel, R. Van Laer, A. H. Safavi-Naeini, Acousto-optic modulation in lithium niobate on sapphire. *APL Photonics* **5**, 086104 (2020). doi: 10.1063/5.0012288
127. W. Jiang *et al*., Efficient bidirectional piezo-optomechanical transduction between microwave and optical frequency. *Nat. Commun.* **11**, 1166 (2020). doi: 10.1038/s41467-020-14863-3; pmid: 32127538
128. K. Buse, A. Adibi, D. Psaltis, Non-volatile holographic storage in doubly doped lithium niobate crystals. *Nature* **393**, 665–668 (1998). doi: 10.1038/31429
129. P. Ying *et al*., Low-loss edge-coupling thin-film lithium niobate modulator with an efficient phase shifter. *Opt. Lett.* **46**, 1478–1481 (2021). doi: 10.1364/OL.418996; pmid: 33720216
130. S. Yang *et al*., Low loss ridge-waveguide grating couplers in lithium niobate on insulator. *Opt. Mater. Express* **11**, 1366 (2021). doi: 10.1364/OME.418423
131. M. Li *et al*., Integrated pockels laser. *Nat Commun* **13**, 5344 (2022). doi: 10.1038/s41467-022-33101-6
132. V. Snigirev *et al*., Ultrafast tunable lasers using lithium niobate integrated photonics. arXiv:2112.02036 [physics. optics] (2021). doi: 10.48550/ARXIV.2112.02036
133. Y. Minet *et al*., Pockels-effect-based adiabatic frequency conversion in ultrahigh-Q microresonators. *Opt. Express* **28**, 2939–2947 (2020). doi: 10.1364/OE.378112; pmid: 32121971
134. M. Jankowski *et al*., Quasi-static optical parametric amplification. *OSA Nonlinear Optics* **2021**, NW3A.1 (2021). doi: 10.1364/NLO.2021.NW3A.1
135. C. Cochard, T. Spielmann, N. Bahlawane, A. Halpin, T. Granzow, Broadband characterization of congruent lithium niobate from mHz to optical frequencies. *J. Phys. D Appl. Phys.* **50**, 36LT01 (2017). doi: 10.1088/1361-6463/aa80b8
136. M. Lee, Dielectric constant and loss tangent in $LiNbO_3$ crystals from 90 to 147 GHz. *Appl. Phys. Lett.* **79**, 1342–1344 (2001). doi: 10.1063/1.1399305
137. A. Herter *et al*., Terahertz waveform synthesis from integrated lithium niobate circuits. arXiv:2204.11725 [physics. optics] (2022). doi: 10.48550/ARXIV.2204.11725
138. Q. Ma, G. Ren, K. Xu, J. Z. Ou, Tunable optical properties of 2D materials and their applications. *Adv. Opt. Mater.* **9**, 2001313 (2021). doi: 10.1002/adom.202001313
139. M. L. Bortz *et al*., Noncritical quasi-phase-matched second harmonic generation in an annealed proton-exchanged $LiNbO_3$ waveguide. *IEEE J. Quantum Electron.* **30**, 2953–2960 (1994). doi: 10.1109/3.362710
140. P. S. Kuo, Noncritical phasematching behavior in thin-film lithium niobate frequency converters. *Opt. Lett.* **47**, 54–57 (2022). doi: 10.1364/OL.444846; pmid: 34951881
141. D. Thomson *et al*., Roadmap on silicon photonics. *J. Opt.* **18**, 073003 (2016). doi: 10.1088/2040-8978/18/7/073003
142. M. Yu *et al*., Femtosecond pulse generation via an integrated electro-optic time lens. arXiv:2112.09204 [physics. optics] (2021). doi: 10.48550/ARXIV.2112.09204
143. T. Vanackere *et al*., "Micro-transfer printing of lithium niobate on silicon nitride" in *2020 European Conference on Optical Communications (ECOC)* (IEEE, 2020).
144. C. Wang *et al*., Ultrahigh-efficiency wavelength conversion in nanophotonic periodically poled lithium niobate waveguides. *Optica* **5**, 1438 (2018). doi: 10.1364/OPTICA.5.001438

**ACKNOWLEDGMENTS**

We thank G. Keeler, S. Diddams, and K. Vahala for discussions and assistance. We also thank many colleagues with whom we have had the privilege to work and learn about the ever-expanding field of LN photonics. We thank Y. Chen for assistance with graph preparations. We also thank J. Rutledge, T. Allison, X. Wu, Y. Li, B. Zhang, and A. Marandi for providing the data for the spectral graphs in Fig. 4. **Funding:** The material is based on work supported by the Australian Research Council (ARC) under awards ARC DP190101576, DP190102773, and DP220100488; the Defense Advanced Research Projects Agency (DARPA) under awards HR0011-20-2-0044, HRO011-15-C-0055, and DARPA-RA-18-02-YFA-ES-578; the National Science Foundation (NSF) under awards CCF-1918549, OIA-2040695, OMA-2137723, and OMA-2138174; the Department of Energy (DOE) under award DE-AC02-76SF00515; the Defense Threat Reduction Agency (DTRA) under award HDTRA11810047; the Beijing Natural Science Foundation under award Z220008; and the National Key Research and Development Program of China under award 2016QY01W0200. **Competing interests:** M.Z. and M.L. are involved in developing LN technologies at HyperLight Corporation and have an equity interest in HyperLight Corporation. M.Z. is an officer and member of the board of directors at HyperLight Corporation. M.Z. and M.L. are named on patents WO2018031916A1, US11092873B1, and WO2020172585A1. M.L. is named on patents US20210223657A1, US20210096444A1, and WO2022115392A1. C.L. and M.F. are named on patent US20220252958A1. 

Submitted 1 July 2022; accepted 3 November 2022
10.1126/science.abj4396